ROYAL SOCIETY
OF CHEMISTRY

PAPER

Check for updates

Efficient single-component nickel catalysts with tetradentate aminopyridine ligands for cycloaddition reactions of CO$_2$ and epoxides under mild conditions†

Congcong Zhang,‡[a] Minghui Shi,‡[a] Ning Yu,[a] Bowen Zhang,*[ab] Feng Han [ID] *[a] and Chengxia Miao [ID] *[a]

A series of single-component nickel catalysts (**L1-NiBr$_2$/L2-NiBr$_2$/L3-NiBr$_2$**) with tetradentate aminopyridine ligands are presented, which exhibit excellent capabilities and selectivity for the synthesis of cyclic carbonates from epoxides and carbon dioxide. A green crystal of **L1-NiBr$_2$** was obtained in CH$_3$CN, and the ligand adopted a *cis-α* conformation in the complex. The conversion of styrene oxide could reach 98%, providing 100% selectivity at 90 °C, 1 MPa CO$_2$ pressure and 5 mol% of **L1-NiBr$_2$** under solvent-free conditions, while the yield and selectivity values were still as high as 92% and 99%, respectively, under 1 atm CO$_2$ and 0.5 mol% of the catalyst at the same temperature. The catalysts also exerted efficient catalytic coupling reactions of terminal epoxides (90–98% yields of cyclic carbonates), except those bearing a long aliphatic chain under mild conditions. The catalyst exhibited excellent recyclability and stability, which were further proved through ICP to test the catalyst leaching, TGA and IR spectra. Moreover, the catalytic cycloaddition reaction mechanism was investigated using density functional theory (DFT) calculations.

Sustainability spotlight

The rapid increase in CO$_2$ emission has had an adverse impact on the environment; therefore, developing sustainable chemical processes to transform CO$_2$ into value-added chemicals is crucial. This study focuses on the production of efficient single-component nickel catalysts with tetradentate aminopyridine ligands and their application for transforming CO$_2$ into cyclic carbonates. The investigation demonstrated that the developed nickel catalysts presented excellent bifunctional catalytic performance, stability and substrate scope under mild conditions, even in low catalyst amounts and atmospheric pressure of CO$_2$ in the absence of solvent, which is industrially attractive for future applications. Our technologies align with the United Nations Sustainable Development Goals, particularly Goals 9, 12 and 13.

1. Introduction

As a potent greenhouse gas, carbon dioxide (CO$_2$) emissions have increased worldwide on a massive scale due to the generation of energy by the combustion of fossil fuels, adversely impacting the environment.[1] Thus, reducing the level of atmospheric CO$_2$ is of utmost importance in the coming decade. In contrast, CO$_2$ is a very significant C1 feedstock in organic synthesis due to its non-flammable, non-toxic, sustainable and inexpensive characteristics.[2] Therefore, the transformation of CO$_2$ into industrially attractive chemicals by chemical strategies has attracted increasing attention.[3] Among them, the production of cyclic carbonates from epoxides and CO$_2$, as an atom-economical reaction, is regarded a considerate method.[4] Moreover, cyclic carbonates have a vibrant area of application in academic and industrial arenas, such as polar aprotic solvents, electrolytes in lithium-ion batteries, and intermediates of biodegradable polymers.[5]

A crucial challenge in the reaction between epoxides and CO$_2$ is the development of suitable catalysts due to the high thermodynamic stability of CO$_2$.[6] To date, numerous catalytic systems, which usually contain both a Lewis acidic center to activate the C–O bond of the epoxide and a Lewis basic site that can be used as a nucleophilic reagent to open the epoxide ring, have been successfully synthesized, including organo-catalysts,[7]

metal complexes catalysts,[8] organic frameworks[9] and others, to catalyze the cycloaddition reaction.[10] Among these active catalytic systems, metal-containing catalysts have attracted increasing attention due to their higher intrinsic Lewis acidity, lower catalyst loadings and lower reaction temperatures.[11] However, most of them are binary catalytic systems, and Lewis bases are usually added as co-catalysts, such as DMAP (4-dimethylaminopyridine) or onium salts.[8c,12] Consequently, considerable efforts to develop efficient one-component bifunctional metal catalyst systems have been proposed to promote cyclic carbonate synthesis without co-catalysts.

As a part of the metal complex, ligands play a pivotal role in developing bifunctional metal catalysts with high catalytic reactivity, and tetradentate nitrogen ligands have been proven efficient for various oxidation reactions, as well as the conversion of CO_2.[13] In view of this, a series of tetradentate aminopyridine-containing metal catalysts have been designed for the transformation of CO_2.[14] For example, various kinds of bifunctional zinc coordination compounds with tetradentate aminopyridine (N4) ligands have been proven efficient catalysts for the coupling reaction between CO_2 and epoxides with a broad substrate scope under solvent-free conditions by Sun et al.[14a] Despite of this, the development of novel N4 bifunctional catalysts under milder conditions is still needed.

In order to achieve the goal, a more active metal center is of utmost importance to obtain high catalytic activity.[15] Nickel (Ni) is inexpensive and earth-abundant, and nickel complexes usually exhibit distinct properties in small molecule activation chemistry and redox chemistry, such as functionalization of alkene and CO_2.[16] Moreover, nickel complexes have been rarely reported for direct coupling of CO_2 with epoxides.[17]

Encouraged by this, metal complexes composed of nickel and N4 were synthesized, and their catalytic activity for the coupling of epoxides and CO_2 to produce cyclic carbonates in the absence of co-catalysts have been evaluated (Scheme 1) and found to be efficient bifunctional catalysts without a co-catalyst.
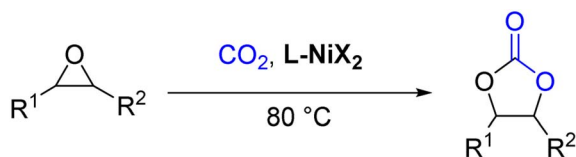
Moreover, a plausible mechanism for the coupling reaction was investigated by density functional theory (DFT).

2. Experimental

2.1 General information

Solvents and chemicals obtained from various companies, such as Aladdin and Macklin, were used without further purification unless stated otherwise. Analytical thin-layer chromatography (TLC) was carried out using 0.25 mm commercial silica gel plates. The purification of product was carried out by flash chromatography using silica gel (200–300 mesh). NMR spectra were performed at 298 K on a Bruker 400. Chemical shift values for ^1H and ^{13}C are reported as δ values (ppm) relative to the deuterated solvent and coupling constants (J) in Hz. Single-crystal X-ray diffraction measurements were carried out on a Bruker Smart APEX II CCD diffractometer at 100 (2) K using Cu Kα radiation ($\lambda = 1.54184$ Å). High-resolution mass spectroscopy experiments were carried out with a Bruker Daltonics microTOF-QII mass spectrometer. The gas chromatography (GC) was recorded by a Shimadzu GC-2010, SE-54 column using diphenyl as the internal standard. Infrared spectra were recorded with a Thermo Scientific Nicolet IS50-IR spectrometer at room temperature.

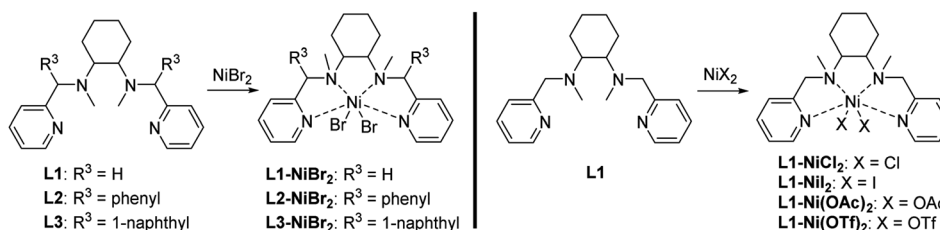### 2.2 Synthesis and characterization of nickel complexes

The ligands **L1–L3** were prepared using previously reported methods.[18]

2.2.1 Synthesis of nickel complexes. An acetonitrile solution of ligand (1.1 mmol) was added dropwise to a stirred solution of $NiBr_2$ (1.0 mmol) or other metal salts in 5 mL anhydrous acetonitrile. The mixture was stirred at 50 °C for 24 h and then cooled to room temperature (Scheme 2). The anhydrous acetonitrile was removed by rotary evaporation, and the solid was washed three times with 15 mL anhydrous ether to obtain the nickel complexes.

2.2.1.1 L1-NiBr₂. Green solid (92%, yield), m. p. 112–114 °C, HRMS (ESI-MS) m/z: calcd for $C_{20}H_{28}BrN_4Ni$ $[M-Br]^+$: 461.0851, found: 461.0845.

2.2.1.2 L2-NiBr₂. Green solid (90%, yield), m. p. 120–122 °C, HRMS (ESI-MS) m/z: calcd for $C_{32}H_{36}BrN_4Ni$ $[M-Br]^+$: 613.1477, found: 613.1473.

2.2.1.3 L3-NiBr₂. Green solid (90%, yield), m. p. 130–132 °C, HRMS (ESI-MS) m/z: calcd for $C_{40}H_{40}BrN_4Ni$ $[M-Br]^+$: 713.1790, found: 713.1786.

Scheme 1 The cycloaddition reaction of CO_2 and epoxides catalyzed by the Ni complex.

Scheme 2 Synthesis of nickel complexes.

2.2.1.4 L1-NiCl₂. Green solid (93%, yield), m. p. 110–112 °C, HRMS (ESI-MS) *m/z*: calcd for $C_{20}H_{28}ClN_4Ni$ $[M–Cl]^+$: 417.1356, found: 417.1350.

2.2.1.5 L1-NiI₂. Green solid (92%, yield), m. p. 110–112 °C, HRMS (ESI-MS) *m/z*: calcd for $C_{20}H_{28}IN_4Ni$ $[M–I]^+$: 509.0712, found: 509.0707.

2.2.1.6 L1-Ni(OTf)₂. Blue solid (90%, yield), m. p. 60–62 °C, HRMS (ESI-MS) *m/z*: calcd for $C_{21}H_{28}F_3O_3SN_4Ni$ $[M-OTf]^+$: 531.1188, found: 531.1182.

2.2.1.7 L1-Ni(OAc)₂. Blue solid (91%, yield), m. p. 60–62 °C, HRMS (ESI-MS) *m/z*: calcd for $C_{22}H_{31}O_2N_4Ni$ $[M–OAc]^+$: 441.1800, found: 441.1795.

2.3 General procedure for the synthesis of cyclic carbonates

Epoxides (1 mmol) and a specified amount of nickel complexes are added to a 25 mL high-pressure vessel along with magnetic particles in the presence of CH_3CN (2 mL) or solvent-free. The internal gas is then replaced with CO_2 three times. The reaction mixture is stirred at the desired temperature for the required time, and the remaining CO_2 is slowly released after cooling the high-pressure vessel to room temperature. The conversion rate of epoxides and the yield of cyclic carbonates are determined by analyzing the crude product with gas chromatography when biphenyl is used as the internal standard. The calculation formula of conversion, yield, selectivity, and TON are given in the ESI.†

3. Results and discussion

The **L1-NiBr₂** powder was dissolved in CH_3CN solution and recrystallized at room temperature for a few days, and then a green crystal was obtained. Its structure was characterized by X-ray diffraction analysis, and the Oak Ridge thermal ellipsoid plot (ORTEP) diagram described in Fig. 1 shows that the ligand coordinated with nickel bromide using four N atoms in a *cis-α* topology. The data collection and structure refinement are
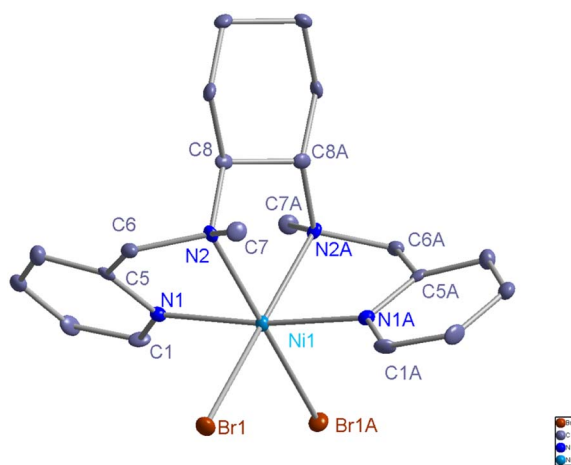
shown in Table S1,† and selected bond lengths and bond angles are summarized in Table S2.†

3.1 Optimization of the reaction conditions

Originally, **L1-NiBr₂** was used to investigate the bifunctional catalytic performance for the coupling reaction of CO_2 and styrene oxide (**1a**) in the presence of 2 mL CH_3CN under the conditions of 2.5 MPa CO_2 and 80 °C for 8 h. It could be seen that the conversion of **1a** and the yield of styrene carbonate (**2a**) were 95% and 94% with the selectivity of 99% when 5 mol% of **L1-NiBr₂** was added alone and no co-catalyst was used, which indicated that **L1-NiBr₂** was an efficient bifunctional catalyst (Table 1, entry 1). Under the same conditions, the effects of common solvents such as CH_3CN, DCE (dichloroethane), toluene, CH_3OH, DMC (dimethyl carbonate), DMF (*N,N*-dimethylformamide), THF (tetrahydrofuran) and solvent-free for the catalytic performance were investigated (Tables S3† and 1, entry 2). The result showed that the catalytic system performed the highest conversion and yield with 100% selectivity in the absence of solvent (Table 1, entry 2). Consequently, the catalytic performance of the cycloaddition between CO_2 and **1a** could be

Table 1 Optimization of the reaction conditions for the catalytic cycloaddition reaction between **1a** and CO_2[a]

Entry	Cat.	*t* (h)	*P* (MPa)	Conv.[b] (%)	Yield[b] (%)	Sel.[b] (%)
1[c]	**L1-NiBr₂**	8	2.5	95	94	99
2	**L1-NiBr₂**	8	2.5	98	98	100
3	**L1-NiBr₂**	4	2.5	99	98	99
4	**L1-NiBr₂**	2	2.5	99	98	99
5	**L1-NiBr₂**	1	2.5	98	98	100
6	**L1-NiBr₂**	0.5	2.5	86	78	91
7	**L1-NiBr₂**	1	1.5	98	98	100
8	**L1-NiBr₂**	1	1.0	98	98	100
9	**L1-NiBr₂**	1	0.5	92	88	96
10	**L1-NiBr₂**	1	0.1	59	57	97
11[d]	**L1-NiBr₂**	1	1.0	51	50	99
12[e]	**L1-NiBr₂**	1	1.0	96	94	98
13[f]	**L1-NiBr₂**	1	1.0	98	97	99
14	**L1-NiCl₂**	1	1.0	85	79	93
15	**L1-NiI₂**	1	1.0	98	96	98
16	**L1-Ni(OAc)₂**	1	1.0	31	—	—
17	**L1-Ni(OTf)₂**	1	1.0	30	—	—
18	**L2-NiBr₂**	1	1.0	95	95	100
19	**L3-NiBr₂**	1	1.0	97	96	99
20	**L1**	1	1.0	8	—	—
21	NiBr₂	1	1.0	22	—	—

[a] Reaction conditions: 1 mmol styrene oxide (**1a**), catalyzed by 5 mol% of catalyst at 80 °C with solvent-free. [b] Determined by gas chromatography using biphenyl as the internal standard. [c] In CH_3CN (2 mL). [d] 1 mol% of **L1-NiBr₂**. [e] 3 mol% of **L1-NiBr₂**. [f] 7 mol% of **L1-NiBr₂**.

Fig. 1 ORTEP diagram of the nickel complex **L1-NiBr₂** (CCDC: 2307070). The hydrogen atoms are omitted for clarity in the metal complex.

optimized without any co-catalyst under solvent-free conditions in the next test.

When the reaction temperature decreased from 80 °C to 60 °C, the conversion of **1a** and the yield of **2a** reduced to 59% and 56%, respectively (Table S4,† entries 1–3). At the same time, the selectivity of the coupling reaction decreased from 100% and 95%, respectively. Increasing the reaction temperature from 80 °C to 90 °C, the conversion and the yield would not decrease, presenting the stability of this catalytic system at higher temperatures (Table S4,† entries 3 and 4). The impact of reaction time on the catalytic performance was next studied with 5 mol% of **L1-NiBr$_2$** as the catalyst at 80 °C under 2.5 MPa CO_2 pressure (Table 1, entries 3–6). Gradually decreasing the reaction time from 8 to 1 h, all of the reactions gave complete conversion from **1a** to **2a**. The conversion and selectivity would be turned to 86% and 91%, respectively, when the reaction time is reduced to 0.5 h. Therefore, 1 h is a more appropriate reaction time for the coupling reaction.
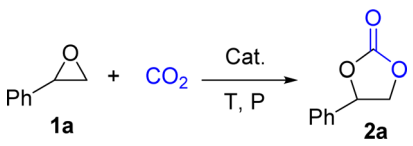
To further investigate more economical reaction conditions, the effect of CO_2 pressure was examined, and good activity could be observed (98% conversion of **1a** and 98% yield of **2a**) under 1 MPa CO_2 (Table 1, entries 7 and 8). However, the conversions of **1a** were 59% and 92%, accompanied by 57% and 88% yields of **2a**, when the CO_2 pressures were 0.1 and 0.5 MPa, respectively (Table 1, entries 9 and 10). Despite the lower conversions of **1a** to **2a**, both presented a satisfactory selectivity (97% at a CO_2 pressure of 0.1 MPa and 96% at a CO_2 pressure of 0.5 MPa) (Table 1, entries 9 and 10). As described in Table 1 (entries 8 and 11–13), the amounts of catalyst were investigated under the conditions of 1 MPa CO_2 and 80 °C for 1 h with **L1-NiBr$_2$** as the catalyst. It could be found that 5 mol% of **L1-NiBr$_2$** was enough to catalyze the coupling reactions of CO_2 with epoxides (Table 1, entry 8).

Then, the activities of several nickel complexes were assessed. Compared to **L1-NiBr$_2$**, **L1-NiCl$_2$** was a little sluggish,

and **2a** was isolated in 79% yield, owing to a lower nucleophilicity of Cl^- (Table 1, entry 14). Although the nucleophilicity of I^- is stronger than Br^-, **L1-NiBr$_2$** showed similar transformation and yield, which may be attributed to the steric hindrance effect of I^- (Table 1, entry 15).[19] However, **2a** was not tested, providing 31% or 30% conversion of **1a** by employing **L1-Ni(OAc)$_2$** or **L1-Ni(OTf)$_2$** as the catalyst, due to the bulky steric hindrance and weak nucleophilicity of OAc^- and OTf^- (Table 1, entries 16 and 17).[20] Besides, 5 mol% of **L2-NiBr$_2$** or **L3-NiBr$_2$** was added into this coupling reaction system to evaluate the effect of the ligand on the catalytic performance under the conditions of 1 MPa CO_2 and 80 °C for 1 h, which also presented satisfactory catalytic ability due to their analogous scaffold (Table 1, entries 18 and 19). The activity of **L-NiBr$_2$** would not be affected by the steric hindrance and electronic property of the ligands. That is to say, anion, as a nucleophilic reagent to open the epoxide ring, played an important role in the reaction. Considering **L1** as a much cheaper ligand than the others, **L1-NiBr$_2$** was the optimized catalyst for the cycloaddition reaction between epoxides and CO_2. When ligand **L1** (5 mol%) or NiBr$_2$ (5 mol%) was added separately for the cyclization reaction, the conversion of **1a** was just 8% or 22% with no **2a** tested in the same conditions (Table 1, entries 20 and 21). The results indicated that there were synergistic catalytic effects between **L1** and NiBr$_2$. After all, one of the optimized conditions is 1 MPa CO_2 pressure and 80 °C for 1 h catalyzed by 5 mol% **L1-NiBr$_2$** under solvent-free.

In order to investigate milder and more commercial reaction conditions, the pressure of CO_2 and the amount of catalyst have been explored. Based on the above-investigated conditions (Table 1, entry 8), the conversion of **1a** was 95%, and the selectivity was about 100% after stirring at 80 °C for 8 h under 1 atm CO_2 (Table 2, entry 1). Consequently, 92% conversion and 92% yield were still obtained when the amount of catalyst decreased to 1 mol% (Table 2, entry 2). With the extension of reaction time, there was no obvious assistance to improve the

Table 2 Investigation of milder conditions for the coupling reaction between **1a** and CO_2 under 1 atm CO_2[a]

Entry	Amount of catalyst (mol%)	t (h)	Conv.[b] (%)	Yield[b] (%)	Sel.[b] (%)	TON
1	5	8	95	95	100	19
2	1	8	92	92	100	92
3	1	12	96	94	98	94
4	0.5	8	65	64	99	128
5	0.5	14	92	91	99	182
6	0.2	12	46	46	100	230
7	0.2	24	76	74	98	370
8[c]	0.5	14	88	85	97	170

[a] Reaction conditions: **1a** (1 mmol), 80 °C, 1 atm CO_2, solvent-free. [b] Gas chromatography is used to determine the conversion rate and yield of cyclic carbonates, with biphenyl as the internal standard. [c] 10 mmol styrene oxide (**1a**).
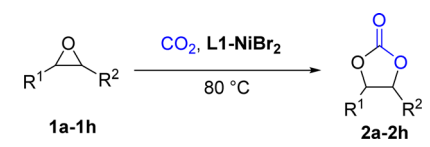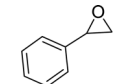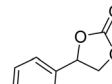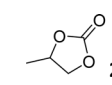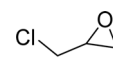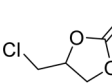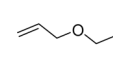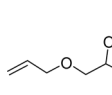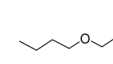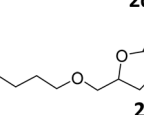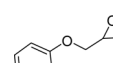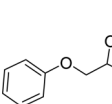
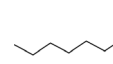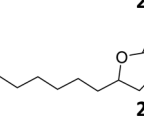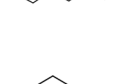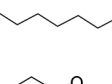yield of **2a** (Table 2, entry 3). In contrast, the conversion of **1a**/ yield of **2a** could be increased from 65%/64% to 92%/91% accompanied by prolonging the reaction time from 8 h to 14 h when the amount of catalyst was 0.5 mol% (Table 2, entries 4 and 5). However, the conversion of **1a** and the yield of **2a** were still less than 80%, even at 80 °C for 24 h at 1 atm CO_2 pressure, when the amount of catalyst reduced to 0.2 mol% (Table 2, entries 6 and 7). In conclusion, the investigated milder reaction conditions were 1 atm CO_2 and 80 °C for 14 h with 0.5 mol% **L1-NiBr$_2$** as the catalyst under solvent-free conditions. It was worth noting that the catalytic system also exhibited great catalytic activity, providing 88% conversion and 85% yield by extending the amount of styrene oxide (**1a**) to 10 mmol (1.20 g) under the optimized conditions (Table 2, entry 8).

The stability of catalyst **L1-NiBr$_2$** was investigated by recycling experiments using **1a** (1 mmol) as the model substrate under 1 atm CO_2 pressure at 80 °C for 14 h with no solvent added. After the first 14 h period, the yield of **2a** was determined by gas spectroscopy, and the reaction mixture was then washed with anhydrous diethyl ether (5.0 mL) to remove **2a** and **1a** and dried. Subsequently, the system was directly added to another 1 mmol **1a** to complete the next circulation. As listed in Fig. 2, this procedure could be repeated five times with almost no loss of its catalytic activity (the yields of **2a** were 92%, 92%, 90%, 91%, and 91%, respectively). The ICP test recorded a 0.76% catalyst leaching in every recycling. The recycling experiments further proved that the catalytic system of **L1-NiBr$_2$** is stable and efficient for the coupling of CO_2 and epoxides under mild conditions. It is worth noting that the stability of **L1-NiBr$_2$** could also be verified by the TGA (thermogravimetric analysis) and IR spectra, which exhibited almost no changes between before and after the cyclic experiment (Fig. S1 and S2†).

3.2 Extend the epoxide substrates

In addition, to investigate the potential and general applicability of the bifunctional catalyst **L1-NiBr$_2$**, the coupling reactions between CO_2 and a variety of epoxides were investigated

Fig. 2 Recyclability of catalyst **L1-NiBr$_2$** for the coupling of CO_2 and **1a** (1 mmol).

Table 3 Substrate scope for cyclic carbonate synthesis

Entry	Epoxide	Product	Yield^{a,b} (%)	Yield^{a,c} (%)
1	**1a**	**2a**	98	91
2	**1b**	**2b**	95	92
3	**1c**	**2c**	97	90
4	**1d**	**2d**	91	95
5	**1e**	**2e**	92	95
6	**1f**	**2f**	92	95
7	**1g**	**2g**	42(95^d)	35
8	**1h**	**2h**	10	6

^{a} Isolated yield. ^{b} Reaction conditions: 1 mmol epoxide, 1 MPa CO_2, 80 °C, 1 h, 5 mol% (relative to the epoxide) **L1-NiBr$_2$**, solvent-free. ^{c} Reaction conditions: 1 mmol epoxide, 1 atm CO_2, 80 °C, 14 h, 0.5 mol% (relative to the epoxide) **L1-NiBr$_2$**, solvent-free. ^{d} 6 h.
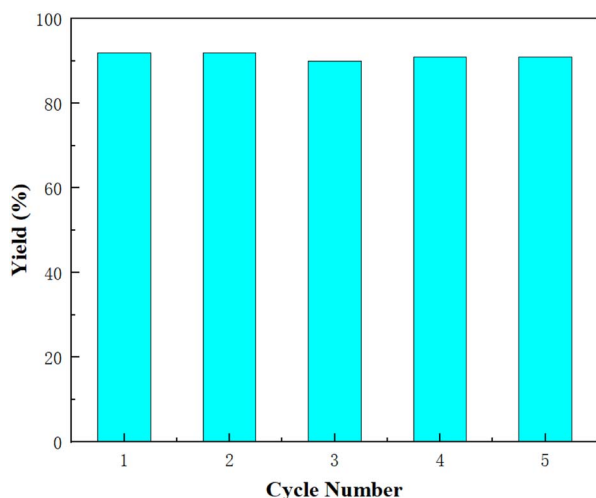
under the above two optimal reaction conditions. It should be noted that **L1-NiBr$_2$** exhibited a good catalytic performance with more than 90% of yield for the transformation of substituted epoxides **1a–1f** bearing various aliphatic and aromatic groups, such as phenyl, methyl, chloromethyl, alkenyl and ether groups under both optimal conditions (Table 3, entries 1–6). However, when the substituted group was a long aliphatic chain, the yields of **2g** decreased to 42% and 35% under the two optimal conditions due to its weak dissolvability for the catalyst (Table 3, entry 7). Fortunately, under the same conditions, increasing the reaction time from 1 h to 6 h, the yield of **2g** would be increased from 42% to 95%. However, the internal epoxide **1h** gave the lowest yield under different reaction conditions due to its steric hindrance (Table 3, entry 8).
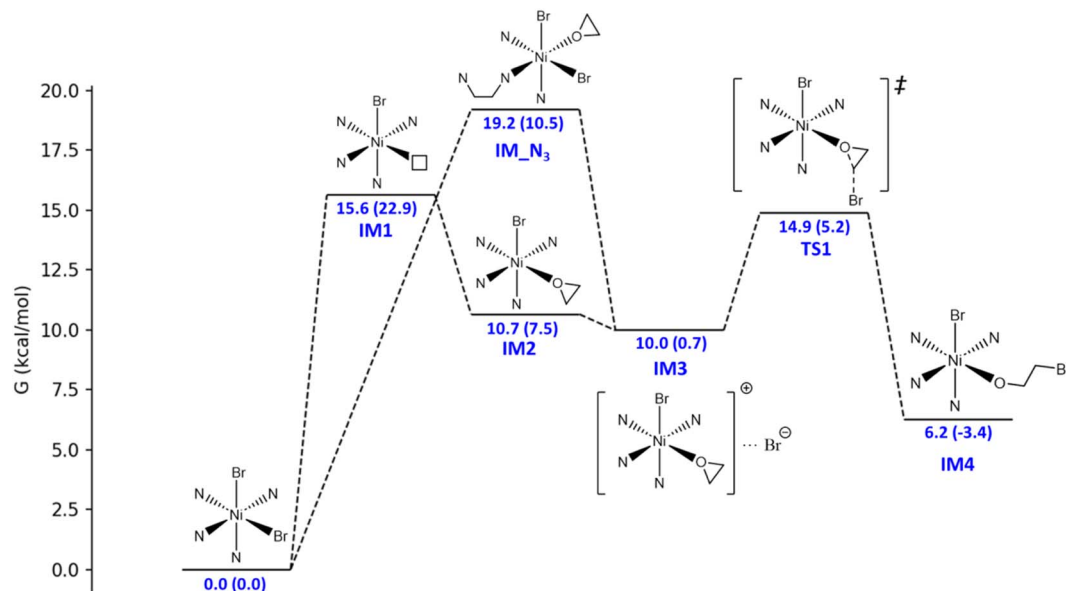
Fig. 3 Energy profile for the binding of the L1-NiBr$_2$ catalyst with the ethylene oxide substrate, followed by the nucleophilic ring opening process. The relative Gibbs free energies and the relative electronic energies (in parentheses) in kcal mol^{-1} are labelled.

3.3 Unravelling the reaction mechanism with DFT calculations

The catalytic mechanism of the coupling reaction of epoxide and CO$_2$ was explored with DFT calculations. Initiation of the catalytic cycle involves a ligand substitution process in which one Br$^-$ leaves the Ni coordination sphere in exchange for an epoxide. Then, the Br$^-$ rebinds to form **IM3** before a nucleophilic attack occurs on the epoxide ring, yielding **IM4** (Fig. 3). A

4.9 kcal mol^{-1} Gibbs free energy barrier was estimated for this ring-opening process. Next, the addition of CO$_2$ occurs, in which the C atom of CO$_2$ weakly binds the O atom originally from the epoxide and currently coordinating to Ni, giving **IM5** (Fig. 4). The insertion of CO$_2$ into the Ni-coordinated bromoethanolate is computed to have a 4.4 kcal mol^{-1} Gibbs free energy barrier. The final step is the ring closure of the bromoethyl carbonate ligand in **IM6**, which is calculated to be the rate-determining step with a Gibbs free energy barrier of
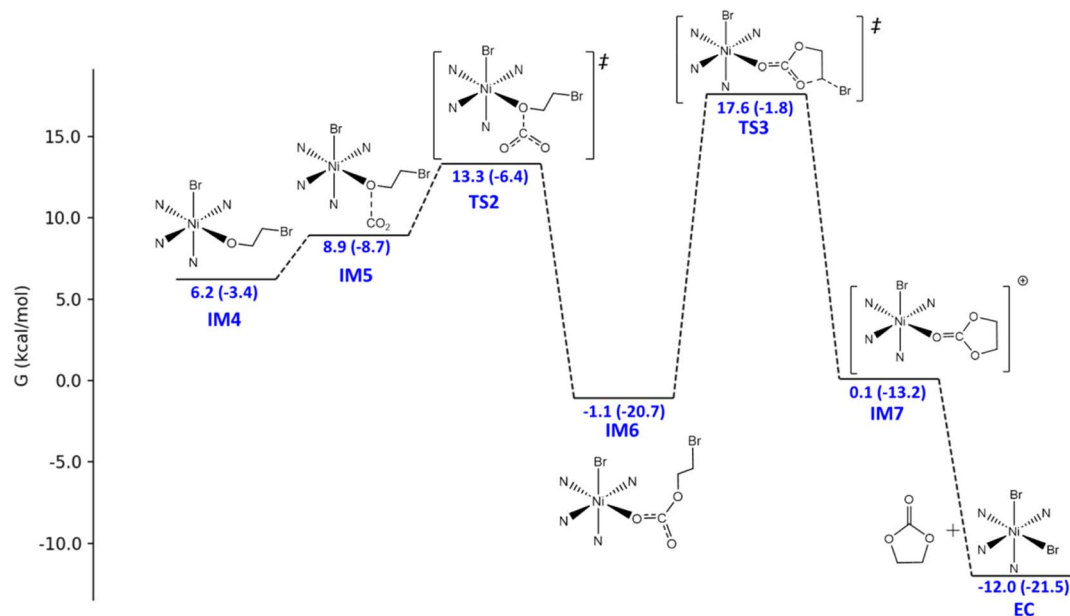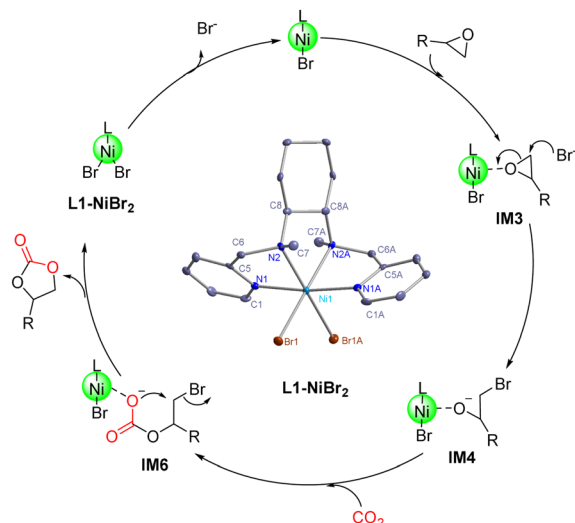

Fig. 4 Energy profile for the conversion from the CoN$_4$BrOCH$_2$CH$_2$Br intermediate (IM4) to the final product, ethylene carbonate (EC). The original L1-NiBr$_2$ catalyst was selected to be the zero-energy scale to stay consistent with Fig. 3. The relative Gibbs free energies and the relative electronic energies (in parentheses) in kcal mol^{-1} are labelled.

Scheme 3 A proposed mechanism for the cycloaddition reaction catalyzed by **L1-NiBr₂**.

18.7 kcal mol⁻¹ (Fig. 4). Releasing the ethyl carbonate molecule closes the catalytic cycle with a net ΔH of -21.5 kcal mol⁻¹. A summary of the proposed reaction mechanism, as per previous reports, is shown in Scheme 3.[21]

4. Conclusion

In summary, novel bifunctional single-component nickel catalysts with tetradentate aminopyridine ligands have been developed for cycloaddition reactions of CO_2 and epoxides. The results indicated that **L1-NiBr₂**, a promising candidate for commercial applications, showed excellent catalytic activity and substrate compatibility under co-catalyst-free and solvent-free conditions. As compared to the disubstituted one, most of the cyclic carbonates achieved high yields (>90%) and selectivity even at 80 °C under 1 atm CO_2 and 0.5 mol% of the catalyst, except the long aliphatic chain substituted one, suggesting that the large epoxide substrates restricted diffusion into the confined spaces of the catalyst. Besides, the developed catalyst has good recyclability and stability, which were further proved through ICP to test the catalyst leaching, TGA and IR spectra. Furthermore, mechanistic investigations followed by DFT suggested that Ni acted as a Lewis acid and its anion Br⁻ acted as a nucleophile to facilitate the ring opening.

Data availability

The data supporting this article have been included as part of the ESI.†

Conflicts of interest

The authors declare that they have no known competing financial interests or personal relationships that could have appeared to influence the work reported in this paper.

Notes and references

1 (*a*) J. Rogelj, D. Huppmann, V. Krey, K. Riahi, L. Clarke, M. Gidden, Z. Nicholls and M. Meinshausen, *Nature*, 2019, **573**, 357–363; (*b*) A. Modak, P. Bhanja, S. Dutta, B. Chowdhury and A. Bhaumik, *Green Chem.*, 2020, **22**, 4002–4033; (*c*) M. Thangamuthu, Q. Ruan, P. O. Ohemeng, B. Luo, D. Jing, R. Godin and J. Tang, *Chem. Rev.*, 2022, **122**, 11778–11829.

2 (*a*) F. Han, F. F. Xie, M. Y. Yin, L. H. Jing and P. Han, *Org. Biomol. Chem.*, 2024, **22**, 5724–5728; (*b*) M. He, Y. Sun and B. Han, *Angew. Chem., Int. Ed.*, 2022, **134**, e202112835; (*c*) Z. Q. Wang, C. H. Deng, X. Liu and W. M. Wang, *Dalton Trans.*, 2023, **52**, 11163–11167.

3 (*a*) A. Goeppert, M. Czaun, J.-P. Jones, G. K. S. Prakash and G. A. Olah, *Chem. Soc. Rev.*, 2014, **43**, 7995–8048; (*b*) Z. C. Zhang, A. Q. Guan, J. Y. Yu, X. D. Jiang, S. Han, Z. Y. Wen, B. Y. Du and B. Y. Song, *New J. Chem.*, 2024, **48**, 13245–13250; (*c*) Q. Zou, G. Long, T. Zhao and X. Hu, *Green Chem.*, 2020, **22**, 1134–1138.

4 (*a*) Z. C. Yang, J. L Ni, C. Y. Duan, Y. Feng and J. F. Yao, *J. Mater. Chem.*, 2024, **12**, 21279–21287; (*b*) Y. Yao, H. Zhang, C. Lu, H. Shang and Y. Tian, *Eur. J. Org Chem.*, 2023, **26**, e202300111.

5 (*a*) B. Schäffner, F. Schäffner, S. P. Verevkin and A. Börner, *Chem. Rev.*, 2010, **110**, 4554–4581; (*b*) W. Yu, E. Maynard, V. Chiaradia, M. C. Arno and A. P. Dove, *Chem. Rev.*, 2021, **121**, 10865–10907; (*c*) A. Centeno-Pedrazo, J. Perez-Arce, Z. Freixa, P. Ortiz and E. J. Garcia-Suarez, *Ind. Eng. Chem. Res.*, 2023, **62**, 3428–3443.

6 P. P. Pescarmona and M. Taherimehr, *Catal. Sci. Technol.*, 2012, **2**, 2169–2187.

7 (*a*) Y. A. Alassmy, Z. A. Pour and P. P. Pescarmona, *ACS Sustainable Chem. Eng.*, 2020, **8**, 7993–8003; (*b*) R. Jin, H. Xu, J. Easa, A. Chapero-Planell and C. P. O'Brien, *J. Phys. Chem.*, 2023, **127**, 1441–1454.

8 (*a*) B.-H. Xu, J.-Q. Wang, J. Sun, Y. Huang, J.-P. Zhang, X.-P. Zhang and S.-J. Zhang, *Green Chem.*, 2015, **17**, 108–122; (*b*) N. H. Kim, E. Y. Seong, J. H. Kim, S. H. Lee, K.-H. Ahn and E. J. Kang, *J. CO₂ Util.*, 2019, **34**, 516–521; (*c*) T. Chuasaard, M. Sinchow, N. Chiangraeng, P. Nimmanpipug and A. Rujiwatra, *J. CO₂ Util.*, 2024, **80**, 102686; (*d*) A. Rehman, F. Saleem, F. Javed, A. Ikhlaq, S. W. Ahmad and A. Harvey, *J. Environ. Chem. Eng.*, 2021, **9**, 105113–105140; (*e*) M. Navarro, A. Garcés, L. F. Sánchez-

Barba, D. González-Lizana and A. Lara-Sánchez, *Dalton Trans.*, 2023, **52**, 6105–6116.

9 (*a*) E. M. Maya, M. González-Lucas and M. Iglesias, *ChemistrySelect*, 2017, **2**, 9516–9522; (*b*) Z. Gao, L. Liang, X. Zhang, P. Xu and J. Sun, *ACS Appl. Mater. Interfaces*, 2021, **13**, 61334–61345.

10 (*a*) Y. Liu, S. Wang, Z. Dai and Y. Xiong, *Ind. Eng. Chem. Res.*, 2021, **60**, 18218–18229; (*b*) Y. L. Hu, X. B. Liu and Q. Rong, *Green Chem. Lett. Rev.*, 2023, **16**, 2163192; (*c*) K. Guo, N. Ji, F. han, Q. Yang, N. Wang and C. Miao, *RSC Sustainability*, 2024, **2**, 1074–1080.

11 (*a*) M. Aresta, A. Dibenedetto and A. Angelini, *Chem. Rev.*, 2014, **114**, 1709–1742; (*b*) C. K. Karan and M. Bhattacharjee, *Inorg. Chem.*, 2018, **57**, 4649–4656; (*c*) J. H. Kim, S. H. Lee, N. H. Kim and E. J. Kang, *J. CO$_2$ Util.*, 2021, **50**, 101595–101601; (*d*) M. Dolai, S. Biswas, E. Moreno-Pineda, W. Wernsdorfer, M. Ali, R. A. Alshgari, S. M. Wabaidur and A. Ghosh, *Cryst. Growth Des.*, 2023, **23**, 801–810.

12 M. H. Chisholm and Z. P. Zhou, *J. Am. Chem. Soc.*, 2004, **126**, 11030–11039.

13 (*a*) H. M. Hüppe, L. I. Mühlhaus, J. Heck, M. Eilers, H. Gildenast, S. Schönfeld, A. Dürrmann, A. Hoffmann, B. Weber, U. P. Apfel and S. H. Pawlis, *Inorg. Chem.*, 2023, **62**, 4435–4455; (*b*) M. Kourgiantaki, G. G. Bagkavou, H. I. Stathakis and A. L. Zografos, *Org. Chem. Front.*, 2023, **10**, 2095–2114; (*c*) B. Wang, X. Cao, L. Wang, X. Meng, Y. Wang and W. Sun, *Inorg. Chem.*, 2024, **63**, 9156–9163.

14 (*a*) B. Wang, L. Wang, J. Lin, C. Xia and W. Sun, *ACS Catal.*, 2023, **13**, 10386–10393; (*b*) J. E. Dengler, M. W. Lehenmeier, S. Klaus, C. E. Anderson, E. Herdtweck and B. Rieger, *Eur. J. Inorg. Chem.*, 2011, **3**, 336–343.

15 (*a*) M. Q. Xing, N. Liu, C. N. Dai and B. H Chen, *Catalysts*, 2024, **14**, 370; (*b*) W. Moschkowitsch, S. Gonen, K. Dhaka, N. Zion, H. Honig, Y. Tsur, M. C. Toroker and L. Elbaz, *Nanoscale*, 2021, **13**, 4576–4584.

16 (*a*) I. Zilbermann, E. Maimon, H. Cohen and D. Meyerstein, *Chem. Rev.*, 2005, **105**, 2609–2625; (*b*) J. Diccianni, Q. Lin and T. N. Diao, *Acc. Chem. Res.*, 2020, **53**, 906–919; (*c*) S. K. Kariofillis and A. G. Doyle, *Acc. Chem. Res.*, 2021, **54**, 988–1000; (*d*) B. H. Teng, Z. P. Bao, Y. Y. Zhao and X. F. Wu, *Org. Lett.*, 2024, **26**, 4779–4783.

17 (*a*) K. Takaishi, B. D. Nath, Y. Yamada, H. Kosugi and T. Ema, *Angew. Chem., Int. Ed.*, 2019, **58**, 9984–9988; (*b*) T. Nouri and M. Khorasani, *J. Phys. Chem.*, 2024, **128**, 166–176.

18 (*a*) M. Wu, B. Wang, S. Wang, C. Xia and W. Sun, *Org. Lett.*, 2009, **11**, 3622–3625; (*b*) S. Yu, C. Miao, D. Wang, S. Wang, C. Xia and W. Sun, *J. Mol. Catal. A: Chem.*, 2012, **353–354**, 185–191.

19 Y. A. Rulev, V. A. Larionov, A. V. Lokutova, M. A. Moskalenko, O. L. Lependina, V. I. Maleev, M. North and Y. N. Belokon, *ChemSusChem*, 2016, **9**, 216–222.

20 Z. Alaji, E. Safaei and A. Wojtczak, *New J. Chem.*, 2017, **41**, 10121–10131.

21 (*a*) F. Chen, Q. Zhang, D. Wei, Q. Bu, B. Dai and N. Liu, *J. Org. Chem.*, 2019, **84**, 11407–11416; (*b*) R. Das and C. M. Nagaraja, *Inorg. Chem.*, 2020, **59**, 9765–9773; (*c*) S. Saltarini, N. V. Escobar, J. Martinez, C. G. Daniliuc, R. A. Matute, L. H. Gade and R. S. Rojas, *Inorg. Chem.*, 2021, **60**, 1172–1182.